Electrical Potential of Leaping Eels

Kenneth C. Catania

Department of Biological Sciences, Vanderbilt University, Nashville, TN, USA

Abstract

When approached by a large, partially submerged conductor, electric eels *(Electrophorus electricus)* will often defend themselves by leaping from the water to directly shock the threat. Presumably, the conductor is interpreted as an approaching terrestrial or semiaquatic animal. In the course of this defensive behavior, eels first make direct contact with their lower jaw and then rapidly emerge from the water, ascending the conductor while discharging high-voltage volleys. In this study, the equivalent circuit that develops during this behavior was proposed and investigated. First, the electromotive force and internal resistance of four electric eels were determined. These values were then used to estimate the resistance of the water volume between the eel and the conductor by making direct measurements of current with the eel and water in the circuit. The resistance of the return path from the eel's lower jaw to the main body of water was then determined, based on voltage recordings, for each electric eel at the height of the defensive leap. Finally, the addition of a hypothetical target for the leaping defense was con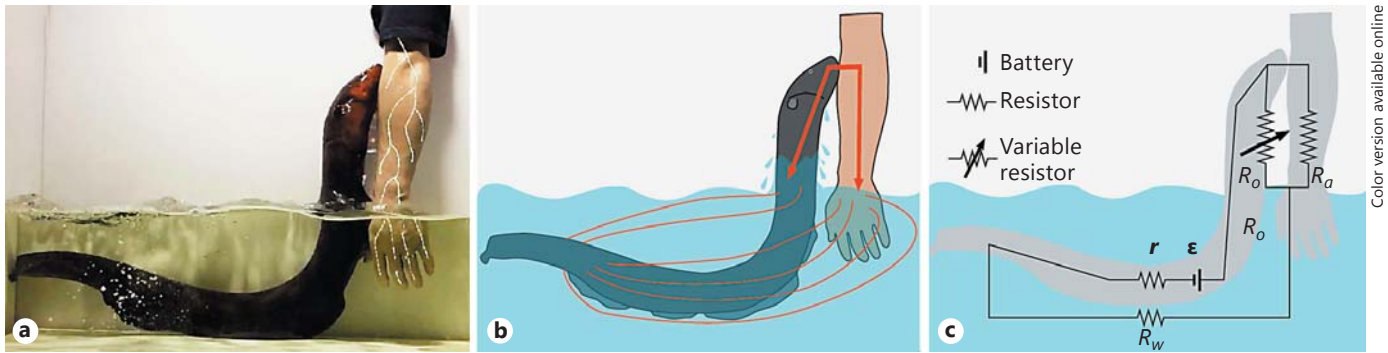sidered as part of the circuit. The results suggest the defensive behavior efficiently directs electrical current through the threat, producing an aversive and deterring experience by activating afferents in potential predators.

© 2017 The Author(s)
Published by S. Karger AG, Basel

Introduction

The long body of an electric eel *(Electrophorus electricus)* is composed primarily of electrogenic tissue, providing this South American fish with the most powerful electrical discharge of any species [Grundfest, 1957]. Large specimens produce discharges of up to 600 V, and when short circuited the external current can be as high as 1 A [Brown, 1950; Coates, 1950]. This ability has made electric eels one of the most famous and long-studied species [Williamson and Walsh, 1775; von Humboldt, 1806, 1807; Faraday, 1832; Du Bois-Reymond, 1849; Sachs, 1881; Coates et al., 1940; Nachmansohn et al., 1943; Albe-Fessard, et al., 1951; Keynes and Martins-Ferreira, 1953; Szabo, 1966; Changeux et al., 1970; Bauer, 1979, Westby, 1988; Gotter et al., 1998; Stoddard, 1999; Stoddard and Markham, 2008; Finger and Piccolino, 2011; Markham, 2013; Gallant et al., 2014; Catania, 2016]. But the impressively large voltages and currents quoted for eels removed from the water in a laboratory setting are not experienced

Kenneth C. Catania
Stevenson Professor of Biological Sciences
Vanderbilt University, VU Station B, Box 35-1634
Nashville, TN 37235 (USA)
E-Mail ken.catania@vanderbilt.edu

Fig. 1. Electric eel defensive behavior. **a** When approached by a relatively large conductor that is partially submerged, electric eels often attack by suddenly leaping from the water while pressing their lower jaw against the threat and discharging high-voltage volleys. In this case, conductive tape on the far side of the arm connects light-emitting diodes (arranged to simulate nerve distributions) to the return path through the water. **b** Schematic illustration of the current paths presumed to develop during the eel's attack. **c** The proposed equivalent circuit that develops as the eel emerges from the water. The electromotive force of the electrocytes is represented by ε. The resistors include water resistance, the eel's internal resistance (r), and the two resistors in parallel. The variable resistor (R_o) represents the current path on, or through, the eel back to the main body of water. This path becomes more resistant as the eel ascends to greater heights. The other resistance (R_a) represents the target. The latter variable is not addressed in the present investigation.

by nearby prey, or potential predators, immersed in the water with the eel. Rather the eel's discharge is distributed throughout the surrounding water, falling rapidly in strength by the effect of geometric spreading [Knudsen, 1975; Hopkins, 1999; Nelson, 2005; Nelson and MacIver, 2006] such that only a small fraction of the power impinges on other animals. Clearly, this fraction is sufficient to act as an efficient means of offense and defense. Indeed, the fact that only a small portion of the eel's output can be conveyed to an aquatic target is the most obvious explanation for the evolution of the eel's prodigious electrical power.

However, the recent discovery of an extraordinary defensive behavior by electric eels, during which they leap from the water to directly electrify threats (Fig. 1), casts the total power output of an eel in a new light [Catania, 2016]. The unattenuated values for whole-body output are, in this case, more directly relevant to the circuit produced. The shocking leap of an electric eel can often be elicited by approaching the eel with a partially submerged, large conductor. In the author's experience, nonconductors do not elicit this defensive behavior. This is consistent with the observation that small conductors are attacked as prey, whereas small nonconductors are ignored [Catania, 2015]. Large conductors are apparently interpreted as large animals. A large partially submerged animal could be a terrestrial predator that had encountered an eel in shallow water [e.g., during the

Amazonian dry season – Catania, 2016]. The leaping defense is not consistent with eel predation because eels never bite at the large conductors during the leap, and eels are gape-limited predators that cannot dismember prey.

In the course of the leaping defense, an eel rises rapidly from the water with its lower jaw in contact with a threatening conductor, while discharging high-voltage volleys. This behavior is shown in Figure 1a, using a prosthetic arm containing eel-powered light-emitting diodes arranged to represent nerve tracts. Figure 1b shows the current flow schematically. Figure 1c shows the proposed equivalent circuit. The equivalent circuit includes the internal resistance of the eel (r), the electromotive force (ε) of the eel's "battery," the resistance of the water in which the eel is immersed (R_w), and two resistors in parallel for the return path of current to the water (R_o and R_a). One of the two latter resistances represents the return path through the small, and decreasing, amount of water on the eel's body as it emerges (R_o). It also includes possible return paths through the eel's internal tissues. Because this resistance increases as the eel attains greater height [Catania, 2016], it is represented as a variable resistor. The other resistance represents the target; in this case the arm (R_a).

In this investigation, experiments were designed to determine the electromotive force (ε) of the eel's summed electrocytes, the internal resistance of the eel (r), the re-
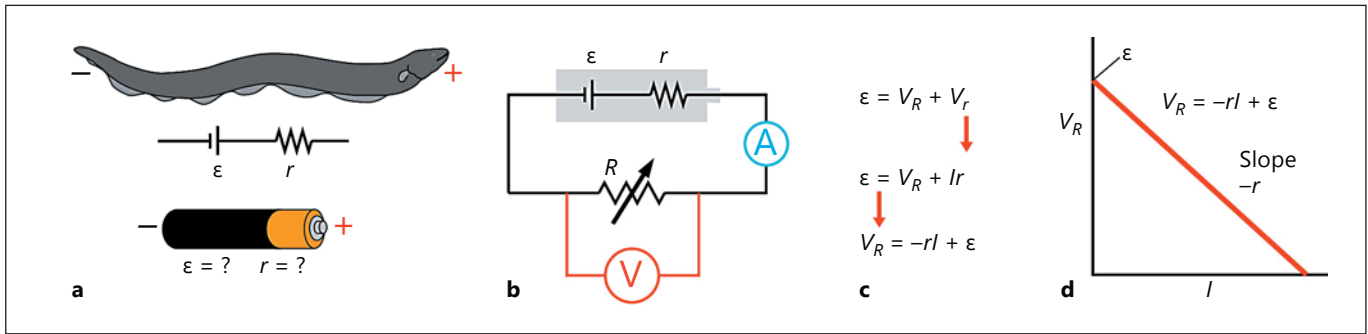
Fig. 2. A method for determining the electromotive force (ε) and internal resistance (r) of a battery. **a** Both electric eel electrocytes and dry-cell batteries are voltage sources and have an internal resistance. **b** Circuit for determining ε and r. Varying the resistance at R results in corresponding changes to the current in the circuit and the voltage drop at each resistor. **c** The voltage drop at the two resistors must add to ε (top), substituting Ir for the last term (middle) allows the equation to be rearranged to plot a straight line (bottom). **d** Plot of the equation in **c** with the voltage drop at R (V_r) plotted on the y axis, I (current) plotted on the x axis, and the negative of the slope equivalent to internal resistance, r.

sistance of the main body of water, and the range of the variable resistor that represents the return path from the eel's lower jaw to the main body of water (Fig. 2). The resistance of the eel's target was not investigated in this study. Results are presented for four different eels ranging in size from approximately 40 cm to over 1 m.

Materials and Methods

All procedures were approved by the Vanderbilt Institutional Animal Care and Use Committee. Eels *(E. electricus)* obtained from commercial fish suppliers were housed in custom-made Plexiglas aquariums ranging in size from 300–480 L with aerated water, gravel bottom, plastic imitation branches, and plants, temperature between 24 and 26°C, pH between 6.5 and 7.0, and conductivity between 100 and 200 μS/cm. Lighting was on a 12-h/12-h light/dark cycle, and eels were fed earthworms and fish. Eel sizes were 40 cm (eel A), 66 cm (eel B), 103 cm (eel C), and 113 cm (eel D).

To record voltage and current directly from the eels, each was lifted into the air in a nonconductive net and contacted at the head and tail with silver-thread-conductive therapy gloves (Conductive Therapy Shop®) worn over rubber gloves. The conductive gloves were in turn connected to 16-G, braided copper speaker wire to form a low-resistance pathway to the remaining circuit elements. The leads from the conductive gloves were connected to an 8-channel, 5-V relay module board for Arduino (JBtek). Five of the 8 relays were used and controlled by a Master-8 stimulator (A.M.P.I., Jerusalem, Israel) that was programmed to sequentially activate the 5 relays at 200-ms intervals (including 200 ms with no relay activated giving 6 conditions). The relays were arranged with resistors to sequentially cycle through open circuit and then approximately 1,600, 800, 400, 200, and 0 Ω. The resistors were 5-W, 200-Ω ceramic resistors (±5% accuracy) that were added together by the relays to produce the values listed above during the experiment.

While the animal was contacted, and the circuit progressed through the resistances as described above, voltage and current (from the eel's high-voltage discharge) were simultaneously measured as illustrated schematically in Figure 3a. Voltage was recorded and stored with both a PowerLab 8/35 data acquisition unit (ADInstruments) through a P4100 100:1 probe (Sainsmart, Lenexa Kansas) using LabChart software (version 7; ADInstruments) at a 100-kHz sampling rate and with a Tektronix TBS 2000 digital oscilloscope through a tuned TPP0100, ×10 attenuating probe at a 100-kHz sampling rate – the latter stored as high-resolution jpegs for each data trace. The dual voltage recordings facilitated figure construction because the PowerLab data traces included all the timing information for the current, voltage, camera, and relay states. However, for convenience, all high-voltage values in the figures and data were taken from the easily tuned attenuating probe of the Tectronix oscilloscope.

Current was measured with a model H1-ACDC-72 (Hall effect) current sensor (BDW Enterprises LLC) at a 100-kHz sampling rate. The current sensor produced a voltage proportional to the current that was in turn recorded on a separate channel of the PowerLab 8/35 data acquisition unit. A known calibrating current (measured by a Fluke 115 True RMS multimeter) was passed through the current sensor and recorded prior to every trial. A third channel of the PowerLab 8/35 data acquisition unit recorded a separate output of the Master-8 stimulator, marking the time during which relays were active.

To convert recorded voltages from the model H1-ACDC-72 current sensor into current measures, the relevant area of the LabChart 7 trace was selected, the "min-max" function was used to record the peak from each discharge using the Datapad function, and these values were exported to Microsoft Excel. The deflection from baseline was converted to current values (amperes) based on the previously recorded calibration current. These data, in addition to the corresponding voltages from the oscilloscope, were imported into the JMP statistical program (a unit of SAS, Cary, NC, USA) to determine standard errors and standard deviations (online suppl. Table 1; see www.karger.com/doi/10.1159/000475743) for each resistance value. The means for each value were plotted
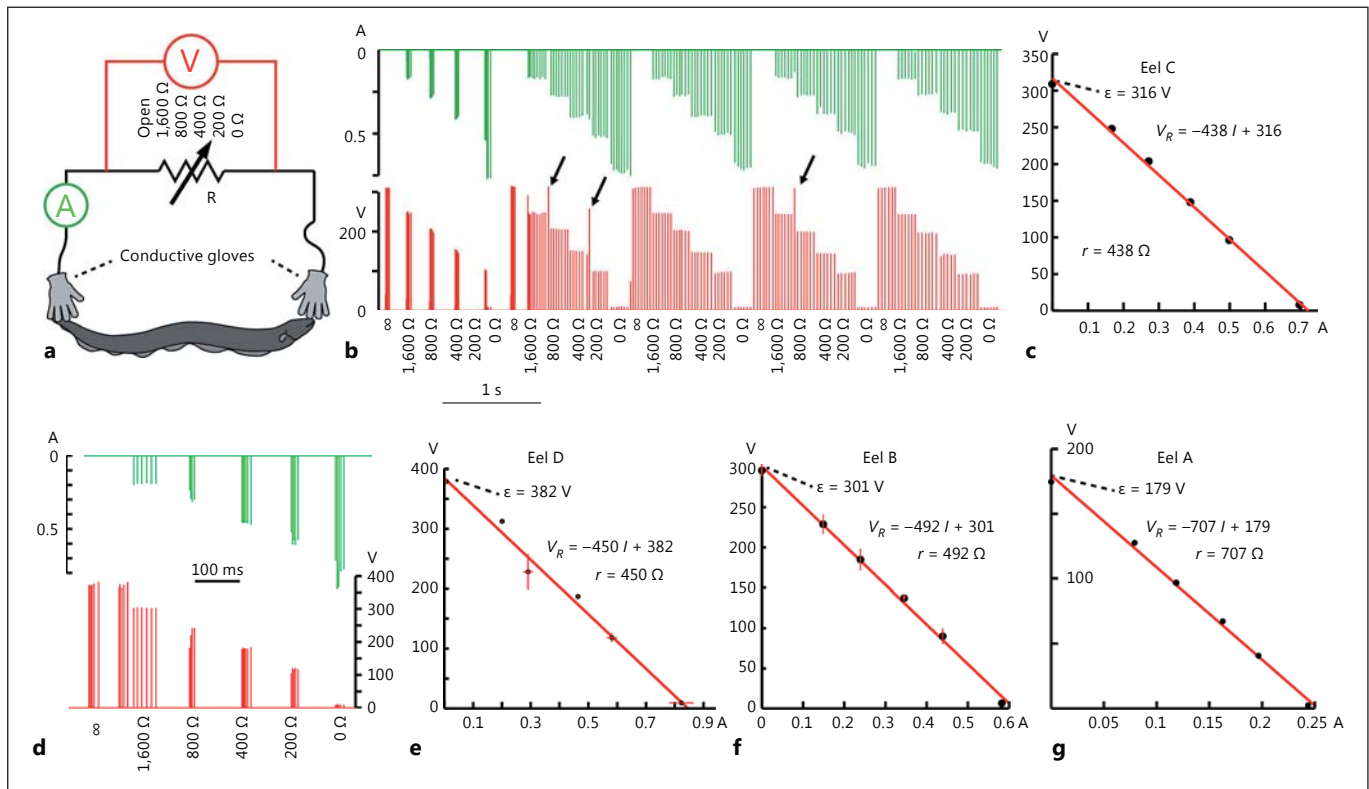
Fig. 3. Determination of electromotive force (ε) and internal resistance (r) for the four eels investigated in this study. **a** Paradigm used to collect voltage and current measurements under 6 different resistance conditions, each lasting 200 ms. Relays cycled through the resistances as the eel was lifted from the water and contacted with conductive gloves. **b** Voltage (red) and current (green) recorded for eel C. This eel began discharging in bursts (leftmost series) and then transitions to a long volley of closely spaced discharges (each eel discharge is monophasic and lasts roughly 2 ms). Some discharges occurred during the short time during which the

relays switched resistors, resulting in occasional "open circuit" conditions between resistor values (arrows). **c** Plot of voltage versus current for each resistor condition for eel C, indicating an electromotive force of 316 V and an internal resistance of 438 Ω. Standard deviations were too small to plot, but are provided in online supplementary Table 1. $R^2 = 0.998$. **d** Voltage versus current plot for eel D. **e** Voltage versus current plot for each resistor condition indicating an electromotive force of 382 V and an internal resistance of 450 Ω. **f, g** Conventions as above for eels B and A.

and a linear fit determined using the "fit line" function, which was used to produce the graphs, and R^2 values, illustrated in Figure 3 and described in the text.

To estimate the value of water resistance, the aquarium water was brought to a conductivity of 100 μS/cm (measured with a calibrated Ohaus Starter 300C conductivity meter accurate to ±0.5%; Ohuas, Parippany, NJ, USA). Four carbon rods (16 cm in length and 1/3 cm in diameter) were positioned vertically at 25-cm intervals (Fig. 4a) by insertion into holes drilled into a Plexiglas holder on the bottom of the aquarium filled to a depth of 30 cm. Each carbon rod was connected by (insulated) 16-G speaker wire to an 8-channel, 5-V relay module board for Arduino controlled by a Master-8 stimulator as described above. Connection points between wire and rod were insulated with moldable plastic. Four relays were used to successively connect one of the rods to a single 16-G wire that ran to a conductive glove as previously described. A net was modified by adding an extension to the bottom that roughly matched the shape and size of the caudal portion of eel C's

body. In this manner, the eel's tail was lowered into the water while each carbon rod was successively switched into the circuit at 250-ms intervals. Current was recorded with a model H1-ACDC-72 (Hall effect) current sensor as described above while the eel was contacted on the head with the conductive glove to complete the circuit. Amperage values were determined from the output of the current sensor as described above. Total resistance for each measure was determined by dividing ε (316 V for eel C) by I (measured for each discharge in the experiment). Water resistance for each distance was determined by subtracting Eel C's internal resistance (438 Ω) from total resistance for each discharge. Results were analyzed in JMP as described above and plotted (with standard deviations shown) in Figure 4c showing water resistance versus distance from the eel's tail for the four carbon rods.

The electric organ discharges were recorded from leaping eels by connecting a split aluminum plate to wires connected to a PowerLab 8/35 data acquisition unit and oscilloscope as described above and illustrated in Figure 5. Water conductivity was 100 μS/
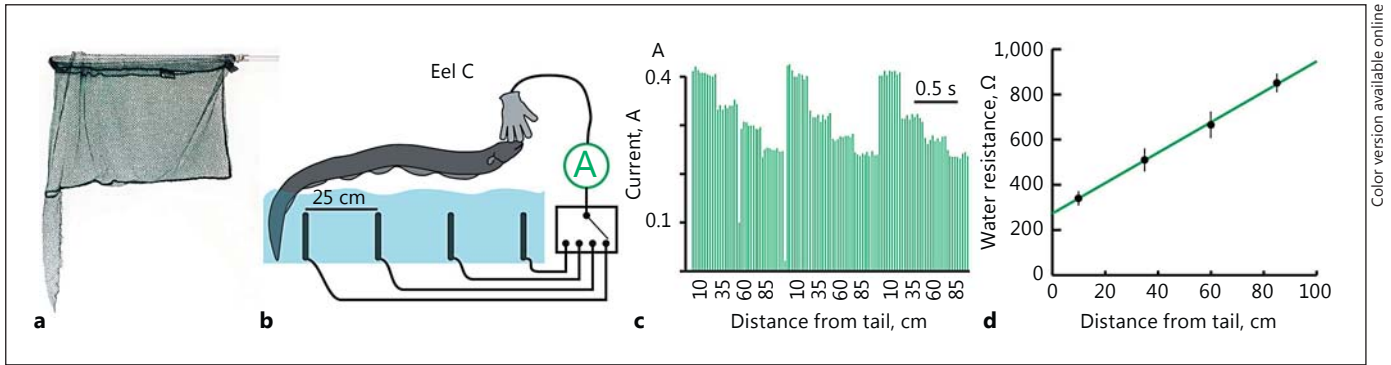
Color version available online

Fig. 4. Method used to estimate the resistance of the water volume between an eel and a conductor. **a** A custom net allowed the tail of eel C to be lowered into the aquarium while the head was contacted with a conductive glove. **b** The relative position of the eel during the recordings. The glove was successively connected (at 250-ms intervals) through relays to carbon rods at fixed distances from the eel's tail. Current was measured for each distance. **c** Current measured for each distance illustrated in **a** for a 3-s interval of continuous discharge. **d** After calculating total resistance of the circuit from the known ε (316 V) and measured I, for each distance, the water resistance was plotted by subtracting the known internal resistance (r) for eel C (438 Ω).

cm. Video was collected with a MotionXtra NX7S1 camera (IDT Inc, Tallahassee, FL, USA) with 2 RPS Studio CooLED 100 RS-5610 for lighting at 1,000 frames/s. The synchronization output of the high-speed camera was recorded on a separate PowerLab channel allowing coordination of video plates and voltage recordings. Voltage values were taken from the oscilloscope as described above. To illustrate the eel's output in relationship to eel behavior, data traces were copied at high resolution from the LabChart 7 program into Adobe Illustrator and illustrated with vector graphics to allow scaling to variable final figure sizes. The waveform for each discharge was replaced with a solid line of equivalent height in the illustrations. Single high-speed video frames that corresponded to eel voltages numbered in Figure 5 were determined from the frame marking TTL recorded by the PowerLab unit.

Results

Eel Electromotive Force and Internal Resistance

Because this investigation bridges the biology of electric eels and the characteristics of the electrical circuit involved, some brief background regarding the basic physical parameters, and method for their measurement, is included and illustrated. Two fundamental characteristics of the eel's discharge are the electromotive force (electrical potential in volts developed by the electrocytes during a discharge [ε]) and the eel's internal resistance to current flow (r). As with a battery, the values of these parameters can be obtained by short circuiting the eel to measure maximal current flow and by separately measuring the maximal voltage developed during a discharge with a high-impedance voltmeter. Internal resistance can

then simply be calculated from V and I by Ohm's law. However, a more accurate value is attained by the experiment illustrated in Figure 2. In this case, an additional resistance is added to the circuit and varied. For each value of resistance, the current and corresponding voltages are recorded and plotted. For internal resistances that follow Ohm's law, a straight line is obtained, with the y-intercept in volts indicating the electromotive force, ε, and the slope equivalent to the negative of the internal resistance (r; Fig. 2c). These values are commonly measured for batteries and have previously been measured for electric eels [Brown, 1950] and other electric fish [Bell et al., 1976; Caputi et al., 1989; Baffa and Correa, 1992]. Previous results indicate that eel electrocytes can be analyzed in this manner as ordinary batteries. Once the values of ε and r have been determined, the values for the other resistances illustrated in Figure 1c can be investigated for any given eel. In the experiments in this study, all voltage and current values refer to the peak value for each of the discharges analyzed, water temperature was 25°C, and water conductivity was 100 μS.

For the present investigation, the technique used was similar to that of the air gap technique of Caputi et al. [1989] but with some modifications. For example, rather than suspending the animal such that only the head and tail were in separate aqueous solutions while the body was in air, or experimenting with an eel on a table [Brown, 1950], the eels were briefly lifted in a nonconductive net and then contacted with soft, conductive gloves connected by wires to the ammeter and voltmeter. This method,

combined with modern multichannel data acquisition units, allowed the voltage and current measurements at different resistances to be obtained in only a few seconds. In addition to reducing stress on the experimental animals, this technique reduced the possibility of electrocyte fatigue that could occur for longer-term experiments.

Figure 3a–c illustrates the paradigm and results for eel C, which provided a remarkably clear, long data set as the eel began discharging in bursts (left-most series in Fig. 3b) and then transitioned to a continuous volley while relays cycled the circuit through 6 different resistances, each lasting 200 ms (for zero resistance, there was some resistance of wires and relays, resulting in a small voltage drop present in "zero" columns; Fig. 3b). Some discharges occurred during the short time during which the relays switched resistors, resulting in occasional "open-circuit" conditions between resistor values (arrows; Fig. 3b). The linear relationship between current and voltage is suggested from the raw data trace (Fig. 3b; amperes in green and volts in red in the online version). A plot of volts versus amperes (Fig. 3c) resulted in a straight line (R^2 = 0.998) with a y-intercept (ε) of 316 V and a slope of –438 (r = 438 Ω).

These results indicate that eel C has an electromotive force of 316 V and an internal resistance of 438 Ω as measured for the peaks of its high-voltage discharge. It should be noted that all electrocytes are active during an eel's high-voltage discharges [Bennett, 1968, 1970]. Thus, electric eels do not have a mechanism to vary the magnitude of their high-voltage discharges during volleys, although it is possible that fatigue causes a reduction in power output over time.

The same experiment was performed for the other 3 eels in the study. Figure 3d, e illustrates the results for a slightly longer eel (eel D). Bursts of high-voltage discharges were more typical of the remaining 3 eels (as illustrated in Fig. 3d), providing fewer data points per unit time than was the case for eel C. Nevertheless, the data were consistent and clear for each animal such that standard errors (and often standard deviations) were too small to illustrate for most points; thus, all bars represent standard deviations. Online supplementary Table 1 provides the number of data points (discharges), standard errors, and standard deviations analyzed for each resistance. For each eel, the relationship between voltage and current was linear, with R^2 values of 0.987, 0.996, and 0.997 for eels D, B, and A, respectively. Thus, values for ε and r were obtained for each specimen. The results showed the expected relationship between longer eel length and greater electromotive force. The eels were la-

beled by increasing length (A–D). Eel A was 40 cm long and eel D was 113 cm long. Values for ε were 179, 301, 316, and 382 V for eels A–D, respectively.

Water Resistance

The resistance of the water surrounding an electric eel is an important variable that affects the circuit developed when an electric eel leaps in self-defense (Fig. 1c). To estimate this resistance, a custom net was designed that allowed current to be measured as the eel's tail was lowered into the water while its head was contacted by a conductive glove (Fig. 4a). The circuit was completed by connecting the glove to one of the four carbon rods submerged in the water at fixed distances from the eel. A series of relays sequentially switch the connection from the glove to one of the carbon rods, progressing from closest to farthest at 250-ms intervals (water was at 25°C and water conductivity was 100 μS/cm). Under these conditions, eel C once again produced a continuous volley of closely spaced, high-voltage discharges (Fig. 4c). Because ε was known for this eel (316 V) and total current (I) was measured in the experiment, total resistance of the circuit was easily determined for each distance ($R = V/I$). Subtracting the known internal resistance for the eel (438 Ω) from total resistance for each carbon rod trial provided the resistance for the water at the different distances from tail to carbon rod (Fig. 4d). This particularly clear data set was used to roughly estimate water resistance for all eels based on approximate distance of the tail from other circuit elements in subsequent analysis and discussion.

Voltages Recorded from Leaping Eels

The next experiment examined the electrical potential (voltage) developed between the lower jaw of the eel and the water as each specimen made shocking leaps. The procedure followed a previously published paradigm [Catania, 2016]. A flat metal plate was divided such that one section could be immersed in the water with only the upper edge protruding. An insulator separated the lower plate from an upper plate; the latter extended well above the water (Fig. 5a). When the lower plate was brought close, the eel usually made an explosive attack. First, contact was made with the lower jaw to the lower plate below the water. Next, the eel followed the lower plate to the water surface and sprang from the water keeping its lower jaw in continual contact as it passed over the insulator and onto the upper plate. Throughout this behavior, a volley of high-voltage discharges was emitted. Voltage was recorded between the two plates as the eel rapidly ascended (Fig. 5). In the course of this behavior, eels often
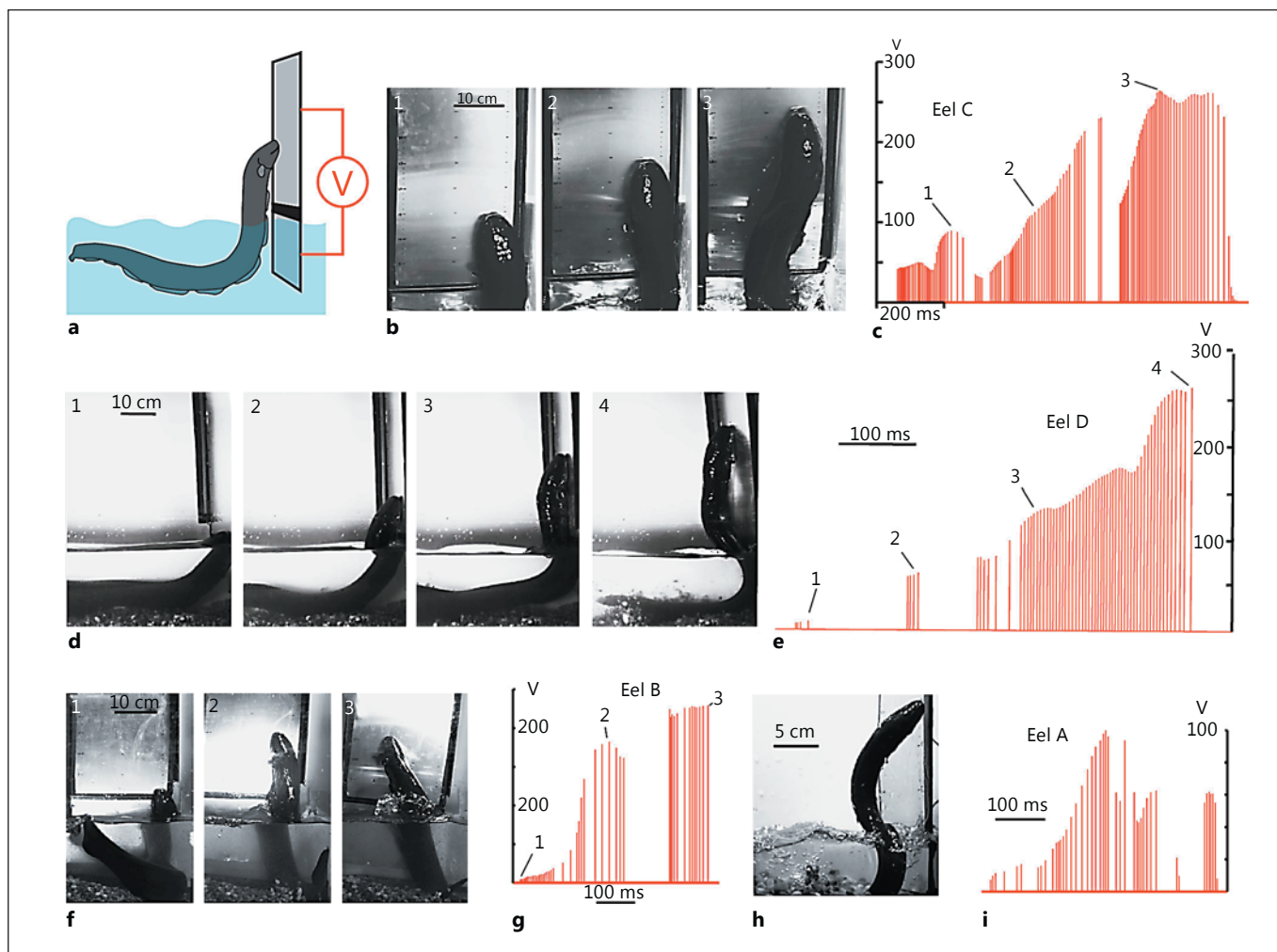
Fig. 5. Measurement of voltage during eel leaping defense. **a** Schematic of the plate arrangement and voltmeter used to measure the electrical potential as eels ascended the conductor. Black line indicates a nonconductor separating the plates. **b**, **d** Frames from high-speed videos for a shocking leap by eel C (**b**) and eel D (**d**). **c**, **e** Voltage measured as eel C (**c**) and eel D (**e**) ascended. Numbers 1–3 correspond the plates illustrated in **b**, and numbers 1–4 correspond to the plates illustrated in **d**, indicating the location of eels C and D at the time of discharge. In these trials, maximum potentials of 265 V (**c**) and 261 V (**e**) were measured. **f–i** Leap and voltage for eel B (**f**, **g**), respectively, and eel A, the smallest eel (**h**, **i**), respectively. **h** The plate is from a different, but similar, trial to that from which voltage was recorded for eel A (**i**).

made various contortions of their anterior body to keep the lower jaw in contact with the plate, thus ensuring the circuit was complete for most of the time the eel's head was above water.

As observed in a previous investigation [Catania, 2016], the recorded voltage increased dramatically as the eels ascended the plate. Initial contact with the upper plate, when most of the eel's body was submerged, corresponded to low-amplitude recordings of only a few volts. Highest-recorded voltages generally corresponded

to the greatest heights reached by the eel on any given trial. In the examples provided in Figure 5, the recorded peaks for eels A, B, C, and D were 100, 228, 265, and 261 V, respectively. These correspond to a substantial proportion of ε for each specimen.

Completing the Circuit

The values for voltages and resistances provided in the experiments described above allow for an approximation of the other components illustrated in Figure 1c and an

estimate of the dynamics of the circuit during the eel's leaping defense. Importantly, the target resistance was not considered in the present analysis. Instead, the circuit elements were considered from the perspective of the voltage recordings from the metal plate during the leap, as measured from a high-impedance voltmeter. Thus, for the conditions of these experiments, the circuit can be considered an unloaded voltage divider.

For brevity, the resulting circuit elements are considered only for eels A and C. In the case of eel C, water resistance was estimated to be 600 Ω, based on the approximate tail distance during the leap illustrated in Figure 5b, c. The peak potential recorded was 265 V (Fig. 5c). Therefore, the voltage drop across the water resistance and internal resistance was ε – 265 V or 51 V. The peak current through the circuit was calculated as 51 V divided by 1,038 Ω (the latter being combined water resistance and internal resistance r) indicating a peak current in the circuit of 0.049 A. From this current, the resistance between the eel's lower jaw and the main body of water could be calculated as $R_0 = V_0/I$ or 265 V/0.049 A $\approx$ 5,400 Ω. Thus, it was estimated that for eel C, the resistance between the lower jaw and the water (for the leap illustrated in Fig. 5b, c) ranged from approximately 0 to 5,400 Ω as the eel ascended (Fig. 6b). Similar calculations can be made for the other eels. For the smallest eel (eel A), the internal resistance, r, was considerably larger at 707 Ω. The water resistance was estimated to be smaller, based on the closer proximity of the tail to the lower plate (400 Ω). The peak potential of 100 V during the leap (Fig. 5h, i) leads to a calculated resistance between lower jaw and water of approximately 0–1,400 Ω as the eel ascended (Fig. 6c).

Discussion

The goal of this study was to first measure the electromotive force (ε) and internal resistance (r) for a number of eels. The next goal was to estimate the additional resistances involved in the circuit that are produced when an eel leaps and shocks in self-defense. These values in turn allow for generalizations to other eels in other settings, electrifying variable targets with different resistances.

The simplified circuit that is proposed to develop when an eel emerges from the water to electrify a threat is illustrated in Figure 1c. It consists of a voltage source (ε), an internal resistance (r), the water resistance (R_w), and two resistors in parallel that form return paths to the water. For the purposes of the present study, the eel's target was

a high-impedance voltmeter. This simplified the measurements to those of an unloaded voltage divider circuit, for which the voltage drop at R_o can be measured as a resistor in series with the remaining components (addition of the target resistance is discussed below).

ε and r for each eel were determined in the manner often used for batteries, and previously used for electric eels [Brown, 1950], and similar to the air gap technique of Caputi et al. [1989]. Total currents and voltages were measured for each eel in a circuit that included an additional resistance that was varied (Fig. 2, 3). A plot of voltage versus current for each resistance value was linear such that the electromotive force and internal resistance could be determined (Fig. 3). The magnitude of ε ranged from 179 V for the smallest (40-cm) eel to 382 V for the longest eel that was over 1 m in length (Fig. 6a). The electromotive force of each eel was roughly proportional to length, as might be expected for the number of electrocytes in series. The lowest internal resistance (438 Ω) was found for the electric eel that clearly had the greatest girth (eel C) rather than the greatest length. This is consistent with the number of electrocytes that might be arranged in parallel. Caputi et al. [1989] found a similar relationship of increasing power output relative to fish size using the air gap technique to investigate *Gymnotus carapo*.

Once ε and r were known, total water resistance was estimated (using a single eel) by directly measuring current in a circuit that included water between the eel's tail and conductive carbon rods at four different fixed distances (Fig. 4). When considering water resistance, it should be noted that the eel's leaping behavior brings its tail and body progressively closer to the target as the eel ascends. This would presumably have the effect of reducing total water resistance as the eel attained greater heights on the target. For this study, a single value of 600 Ω was used for eel C, whereas a single value of 400 Ω was used for eel A (the smallest eel). Relatively large (percentage) changes to this value would have little effect on the calculation of return path resistance (see below).

Measurement of the voltage drop across the final resistance to be analyzed was facilitated by the nature of the eel's leaping behavior, during which each specimen voluntarily connects itself to a voltmeter through the conductive plate arrangement illustrated in Figure 5a. High-speed video recordings, coordinated with voltage recordings, allowed for a comparison between eel height and electrical potential during this behavior. Kirchhoff's voltage law (the sum of the voltage drops in the circuit must add to zero) allowed subsequent calculation of this resistance by subtraction of the other components, as outlined
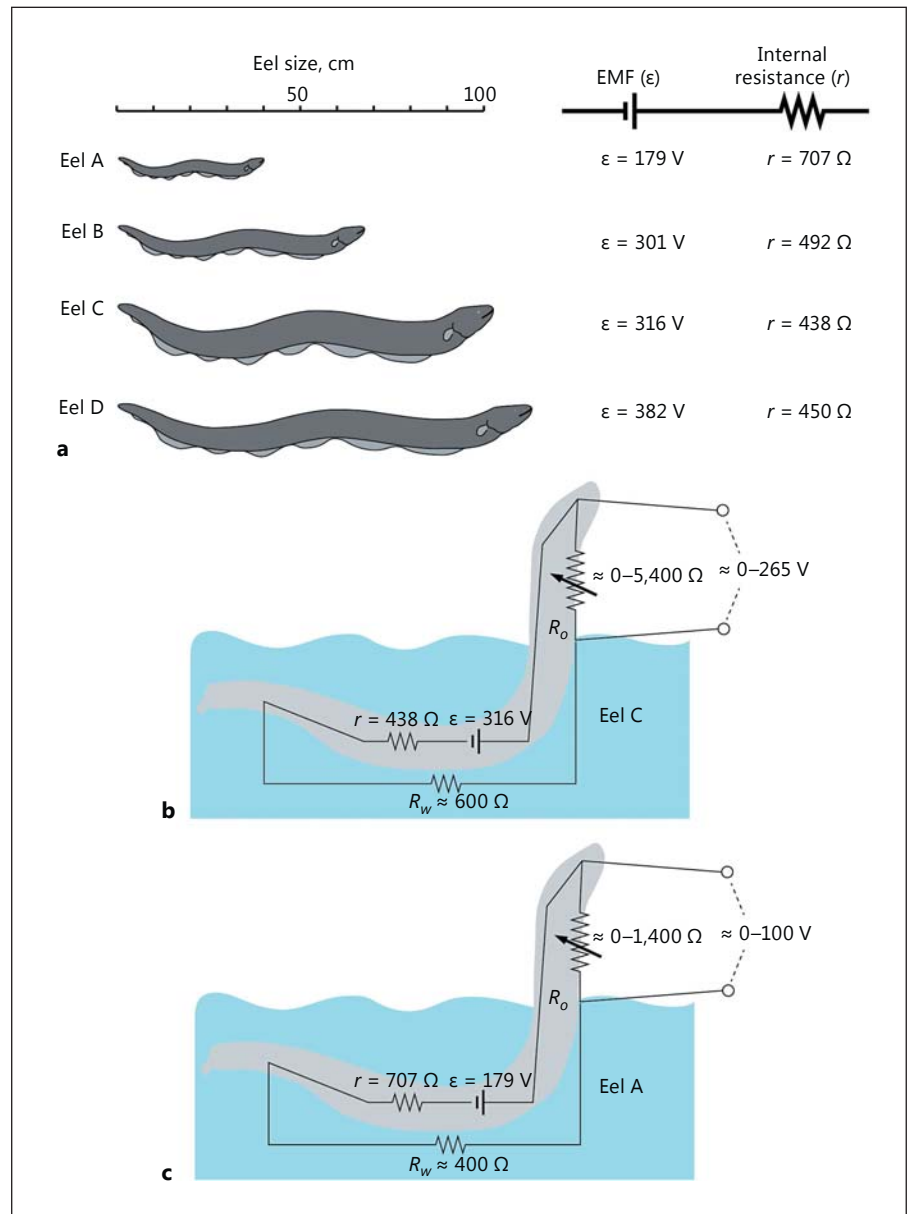
Fig. 6. Summary of electromotive force (EMF; ε) internal resistance (r), and estimated resistances in the circuit during eel leaping defense. **a** Size of each eel in relationship to ε and r. **b**, **c** Estimate of water resistance (from data in Fig. 4) and the maximum resistance of the return path to the water during the leap by eel C (**b**), as illustrated in Figure 5b, c, and eel A (**c**), as illustrated in Fig. 5h, i. The smaller water resistance corresponds to the shorter distance from tail to conductor in the leaping trial. These summaries present the eels' circuit as an unloaded voltage divider in the absence of a target resistance and current path (see text).

in the results. The results indicated that the resistance between the eel's lower jaw and the main body of water increases from (presumably) zero to thousands of ohms as the eel ascends. The examples included in this study reflect the maximum voltage attained from only a few trials for each animal. There is little doubt the resistance of the return path over or through the eel's body may be considerably greater for higher leaps. For example, in the course of observing and photographing eels leaping at diverse stimuli, some instances include examples for which the eel comes most of the way out of the water (Fig. 7). It is

possible that eels curtail the behavior when very high resistance is encountered (as in the case of the high-impedance voltmeter, for which negligible current flows between the upper and lower plates). The examples shown in Figure 7 were cases for which current flowed through conductive tape on the prop, through light-emitting diodes, and then through a return path to the water. Feedback to the eel about this completed circuit could indicate a successful, on-target electrification of the threat and hence result in a longer and higher leap. More studies are needed to explore this possibility. But regardless of poten-
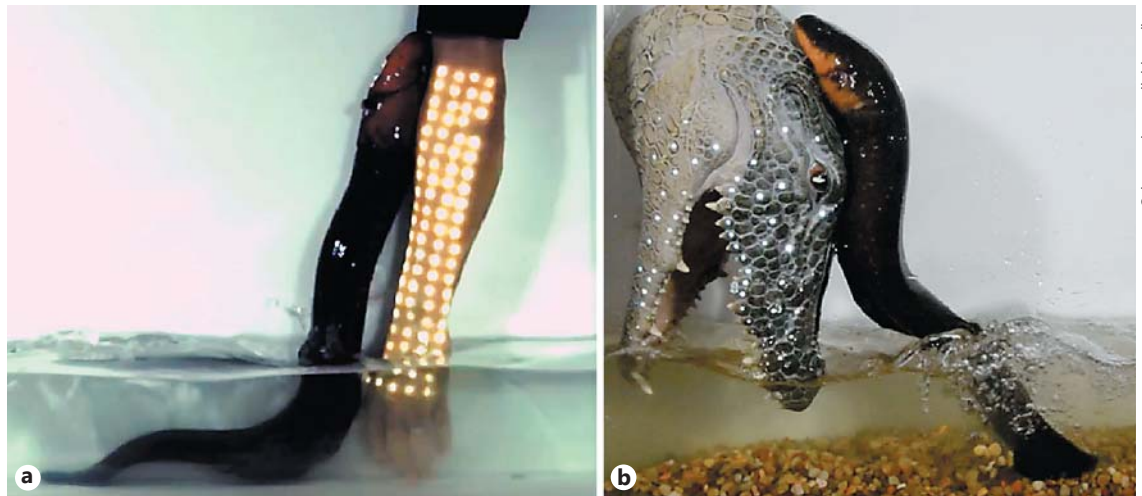
Fig. 7. Examples of electric eel leaps during which a large proportion of the eel's body emerges from the water. **a**, **b** In these trials, the circuit to the water (through light-emitting diodes) was connected to allow for substantial current flow during the behavior.
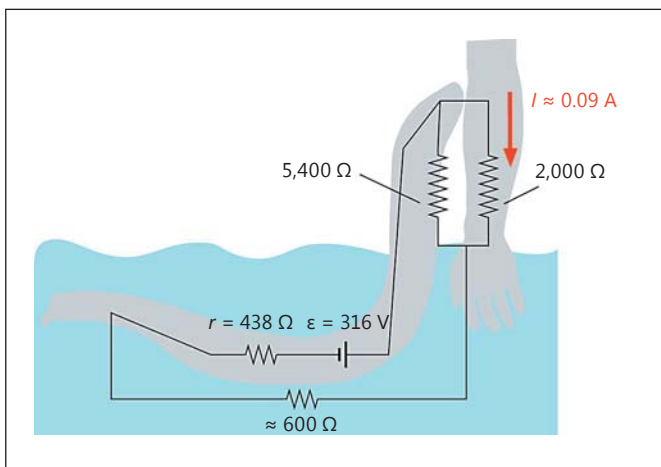
Fig. 8. The proposed circuit that would develop when an eel emerges from the water to electrify a human arm. Values for eel electromotive force and related resistances are taken from data for eel C; the resistance of the human arm was estimated from Reilly [2012].

tial feedback to the eel, greater heights (Fig. 7) would be expected to correspond to greater resistances for the return path than illustrated in Figure 6b, c. Thus, peak resistance values from 5,000–8,000 Ω might be predicted for large electric eels that had risen to half their body length during a shocking leap.

Having explored the electrical circuit involved when an eel leaps in self-defense, the next obvious question is how

this circuit affects the target at which the eel is directing its high voltage? This is the case for the complete circuit illustrated in Figure 1c, for which two resistors are in parallel. It represents a current divider circuit, and it is obvious that more current will flow through the path of least resistance. This provides the basis for the selection of the eel's leaping behavior, which progressively decreases the *relative* resistance of the target as the eel ascends to greater heights (one assumption for this conclusion is that electric eels do not have low-resistance tissues that form an internal return pathway for the electrocytes, as this would make their use of high-voltage discharges unfeasible in general). The familiar formula for determining current through each resistor in parallel is $I_N = I_{Total} (R_{Total}/R_N)$.

It is perhaps most informative to consider an example. If we assume a wet human arm (as would inevitably be the case at the contact point between an eel and its target) has a resistance of 2,000 Ω [Reilly, 2012], then a large eel would impart most of the current in the circuit through the human limb at peak height. In the case of eel C, as illustrated for Figure 8, roughly 0.09 A of current would flow through the arm, equivalent to 16 W, in brief pulses corresponding to the peak of each high-voltage discharge. A pulse rate of 200–300 Hz has been used in numerous studies to activate nociceptors in diverse species [Duranti et al., 1983; Anderson et al., 1999; Arendt-Nielsen et al., 2000; Spadavecchia et al., 2002; Kimura et al., 2004] – similar to the eel's high-voltage discharge rate while leaping. Moreover, when humans were stimulated at 300 Hz,

pain threshold was reached at a current of roughly 5 mA, with very severe pain at 18 mA. Clearly, 90 mA would cause considerable pain.

It is not clear which potential predators may have led to the evolution of the defensive behavior, or what the particular resistance of the predator's epidermis might be. In a previous report [Catania, 2016], the author reported that eels over 60 cm engaged in this behavior. In the present study, it was discovered that all eels examined over the length of approximately 30 cm (6 juvenile specimens) engaged in the behavior. The behavior was exhibited in full form from these growing juveniles when first observed, but a precise developmental stage at which it emerged was not recorded. Nevertheless, it is clearly a common and in-

nate behavior. It seems most likely that the function of the high-voltage discharges, during shocking leaps, is to activate afferents that would result in a highly aversive experience for potential predators on the receiving end.

Disclosure Statement

The author has no conflict of interests to declare.

References

Albe-Fessard D, Chagas C, Couceiro A, Fessard A (1951): Characteristics of responses from electrogenic tissue in *Electrophorus electricus*. J Neurophysiol 14:243–252.

Andersen OK, Sonnenborg FA, Arendt-Nielsen L (1999): Modular organization of human leg withdrawal reflexes elicited by electrical stimulation of the foot sole. Muscle Nerve 22:1520–1530.

Arendt-Nielsen L, Sonnenborg FA, Andersen OK (2000): Facilitation of the withdrawal reflex by repeated transcutaneous electrical stimulation: an experimental study on central integration in humans. Eur J Appl Physiol 81:165–173.

Baffa O, Correa SL (1992): Magnetic and electric characteristics of the electric fish Gymnotus carapó. Biophys J 63:591–593.

Bauer R (1979): Electric organ discharge (EOD) and prey capture behaviour in the electric eel, *Electrophorus electricus*. Behav Ecol Sociobiol 4:311–319.

Bell CC, Bradbury J, Russell CJ (1976): The electric organ of a mormyrid as a current and voltage source. J Comp Physiol A Neuroethol Sens Neural Behav Physiol 110:65–88.

Bennett MVL (1968): Neural control of electric organs; in Ingle D (ed): The Central Nervous System and Fish Behavior. Chicago, University of Chicago Press, pp 147–169.

Bennett MVL (1970): Comparative physiology: electric organs. Annu Rev Physiol 32:471–528.

Brown MV (1950): The electric discharge of the electric EEL. Elect Eng 69:145–147.

Caputi A, Macadar O, Trujillo-Cenóz O (1989): Waveform generation of the electric organ discharge in *Gymnotus carapo*. J Comp Physiol A Neuroethol Sens Neural Behav Physiol 165:361–370.

Catania KC (2015): Electric eels use high-voltage to track fast-moving prey. Nat Commun 6:8638.

Catania KC (2016): Leaping eels electrify threats, supporting Humboldt's account of a battle with horses. Proc Natl Acad Sci USA 113:6979–6984.

Changeux J-P, Kasai M, Lee C-Y (1970): Use of a snake venom toxin to characterize the cholinergic receptor protein. Proc Natl Acad Sci USA 67:1241–1247.

Coates CW, Cox RT, Rosemblith WA, Brown MB (1940): Propagation of the electric impulse along the organs of the electric eel, *Electrophorus electricus* (Linnaeus). Zoologica 25(pt 2).

Coates CW (1950): Electric fishes. Elect Eng 69:47–51.

Du Bois-Reymond E (1849): Untersuchungen über tierische Elektrizität. Berlin, Reimer.

Duranti R, Galletti R, Pantaleo T (1983): Relationships between characteristics of electrical stimulation, muscle pain and blink responses in man. Electroencephalogr Clin Neurophysiol 55:637–644.

Faraday M (1832): Experimental researches in electricity. Phil Trans R Soc Lond 122:125–162.

Finger S, Piccolino M (2011): The shocking history of electric fishes: from ancient epochs to the birth of modern neurophysiology. Oxford, Oxford University Press, p 5.

Gallant JR, Traeger LL, Volkening JD, Moffett H, Chen PH, Novina CD, Phillips GN Jr, Anand R, Wells GB, Pinch M, Güth R, Unguez GA, Albert JS, Zakon HH, Samanta MP, Sussman MR (2014): Nonhuman genetics. Genomic basis for the convergent evolution of electric organs. Science 344:1522–1525.

Gotter AL, Kaetzel MA, Dedman JR (1998): *Electrophorus electricus* as a model system for the study of membrane excitability. Comp Biochem Physiol A Mol Integr Physiol 119:225–241.

Grundfest H (1957): The mechanisms of discharge of the electric organs in relation to general and comparative electrophysiology. Prog Biophys Biophys Chem 7:1–85.

Hopkins CD (1999): Design features for electric communication. J Exp Biol 202:1217–1228.

Keynes RD, Martins-Ferreira H (1953): Membrane potentials in the electroplates of the electric eel. J Physiol 119:315.

Kimura S, Honda M, Tanabe M, Ono H (2004): Noxious stimuli evoke a biphasic flexor reflex composed of Aδ-fiber-mediated short-latency and C-fiber-mediated long-latency withdrawal movements in mice. J Pharmacol Sci 95:94–100.

Knudsen EI (1975): Spatial aspects of the electric fields generated by weakly electric fish. J Comp Physiol 99:103–118.

Markham MR (2013): Electrocyte physiology: 50 years later. J Exp Biol 216:2451–2458.

Nachmansohn D, Cox RT, Coates CW, Machado AL (1943): Action potential and enzyme activity in the electric organ of *Electrophorus electricus*. II. Phosphocreatine as energy source of the action potential. J Neurophysiol 6:383–396.

Nelson ME (2005): Target detection, image analysis, and modeling; in Bullock TH, Hopkins CD, Popper AN, Fay RR (eds): Electroreception. New York, Springer, pp 290–317.

Nelson ME, MacIver MA (2006): Sensory acquisition in active sensing systems. J Comp Physiol A 192:573–586.

Reilly JP (2012): Applied Bioelectricity: From Electrical Stimulation to Electropathology. New York, Springer Science & Business Media, 2012, pp 20–42.

Sachs C (1881): Untersuchungen am Zitteraal, *Gymnotus electricus*. Nach seinem Tode bearbeitet von Emil du Bois-Reymond. Leipzig, Veit.

Spadavecchia C, Spadavecchia L, Andersen OK, Arendt-Nielsen L, Leandri M, Schatzmann U (2002): Quantitative assessment of nociception in horses by use of the nociceptive withdrawal reflex evoked by transcutaneous electrical stimulation. Am J Vet Res 63:1551–1556.

Stoddard PK (1999): Predation enhances complexity in the evolution of electric fish signals. Nature 400:254–256.

Stoddard PK, Markham MR (2008): Signal cloaking by electric fish. Bioscience 58:415–425.

Szabo T (1966): The origin of electric organs of *Electrophorus electricus*. Anat Rec 155:103–110.

von Humboldt A (1807): Jagd und Kampf der elektrischen Aale mit Pferden. Aus den Reiseberichten des Hrn. Freiherrn Alexander v. Humboldt. Ann Physik 25:34–43.

von Humboldt A (1806): Versuche über die elektrischen Fische. Ann Physik 22:1–13.

Westby GM (1988): The ecology, discharge diversity and predatory behaviour of gymnotiforme electric fish in the coastal streams of French Guiana. Behav Ecol Sociobiol 22:341–354.

Williamson H, Walsh J (1775): Experiments and Observations on the *Gymnotus electricus*, or electrical eel. Philos Transact 65:94–101.